THE FASEB JOURNAL • RESEARCH • www.fasebj.org

Fas receptor induces apoptosis of synovial bone and cartilage progenitor populations and promotes bone loss in antigen-induced arthritis

Elvira Lazić Mosler,[*,†,‡,1] Nina Lukač,[*,§,1] Darja Flegar,[*,¶] Martina Fadljević,[*] Igor Radanović,[*] Hrvoje Cvija,[*] Tomislav Kelava,[*,¶] Sanja Ivčević,[*,‖] Alan Šućur,[*,¶] Antonio Markotić,[*,#] Vedran Katavić,[*,§] Ana Marušić,[**] Danka Grčević,[*,¶] and Nataša Kovačić[*,§,2]

[*]Laboratory for Molecular Immunology, Croatian Institute for Brain Research, [§]Department of Anatomy, and [¶]Department of Physiology and Immunology, University of Zagreb School of Medicine, Zagreb, Croatia; [†]Department of Dermatology and Venerology, General Hospital Dr. Ivo Pedišić, Sisak, Croatia; [‡]Department of Nursing, Catholic University of Croatia, Zagreb, Croatia; [‖]Huntsman Cancer Institute, University of Utah, Salt Lake City, Utah, USA; [#]Centre for Clinical Pharmacology, University Clinical Hospital Mostar, Mostar, Bosnia and Herzegovina; and [**]Department of Research in Biomedicine and Health, University of Split School of Medicine, Split, Croatia

ABSTRACT: Rheumatoid arthritis (RA) is inflammatory joint disease that eventually leads to permanent bone and cartilage destruction. Fas has already been established as the regulator of inflammation in RA, but its role in bone formation under arthritic conditions is not completely defined. The aim of this study was to assess the effect of Fas inactivation on the bone damage during murine antigen-induced arthritis. Subchondral bone of wild-type (WT) and Fas-knockout ($Fas^{-/-}$) mice was evaluated by histomorphometry and microcomputerized tomography. Proportions of synovial bone and cartilage progenitors were assessed by flow cytometry. Synovial bone and cartilage progenitors were purified by fluorescence-activated cell sorting and expression of Fas and Fas-induced apoptosis were analyzed *in vitro*. Results showed that $Fas^{-/-}$ mice developed attenuated arthritis characterized by preserved epiphyseal bone and cartilage. A proportion of the earliest $CD200^+$ bone and cartilage progenitors was reduced in WT mice with arthritis and was unaltered in $Fas^{-/-}$ mice. During osteoblastic differentiation *in vitro*, $CD200^+$ cells express the highest levels of Fas and are removed by Fas ligation. These results suggest that Fas-induced apoptosis of early $CD200^+$ osteoprogenitor population represents potential mechanism underlying the impaired bone formation in arthritis, so their preservation may represent the bone-protective mechanism during arthritis.—Lazić Mosler, E., Lukač, N., Flegar, D., Fadljević, M., Radanović, I., Cvija, H., Kelava, T., Ivčević, S., Šućur, A., Markotić, A., Katavić, V., Marušić, A., Grčević, D., Kovačić, N. Fas receptor induces apoptosis of synovial bone and cartilage progenitor populations and promotes bone loss in antigen-induced arthritis. FASEB J. 33, 000–000 (2019). www.fasebj.org

KEY WORDS: mesenchymal cells · osteoprogenitors · osteoblasts · rheumatoid arthritis

Rheumatoid arthritis (RA) is a systemic, autoimmune disease, characterized by symmetric polyarthritis, which eventually results in permanent disability from the destruction of articular cartilage and underlying bone. The main characteristic of RA is synovial thickening from uncontrolled fibroblast-like synoviocyte (FLS) proliferation, accompanied by infiltration of the synovium by lymphocytes, macrophages, and neutrophils (1). Infiltrating cells, as well as proliferating FLS, produce proinflammatory cytokines, such as TNF, IL-1, -6, -7, -8, -15, -17, -18, -32, and -35, and IFNs (2–10). In addition to their role in initiating and supporting inflammation, these cytokines also contribute to bone damage by affecting the balance between osteoclastic bone resorption and osteoblastic bone formation (11, 12). Many of the mentioned cytokines affect homing and activation of osteoclast progenitors or

ABBREVIATIONS: 7-AAD, 7-aminoactinomycin D; AF488, Alexa Fluor 488; AIA, antigen-induced arthritis; AP, alkaline phosphatase; APC, allophycocyanin; *bglap*, bone γ-carboxyglutamate protein, osteocalcin gene; BV/TV, bone volume/total volume; *Col*α*2*, collagen type I, α2 chain; FACS, fluorescence-activated cell sorting; $Fas^{-/-}$, Fas knockout; FasL, Fas ligand; FLS, fibroblast-like synoviocyte; i.a., intraarticular; IQR, interquartile range; *lpr*, lymphoproliferative syndrome; mBSA, methylated bovine serum albumin; MB, methylene blue; μCT, microcomputerized tomography; NI, nonimmunized; OPG, osteoprotegerin; PE, phycoerythrin; PECy7, phycoerythrin-cyanine 7; PI, propidium iodide; RA, rheumatoid arthritis; RANKL, receptor activator of nuclear factor κB ligand; *Runx2*, runt-related transcription factor 2; SSC, skeletal stem cell; Tb.N, trabecular number; Tb.Sp, trabecular separation; Tb.Th, trabecular thickness; WT, wild type

[1] These authors contributed equally to this work.

[2] Correspondence: Department of Anatomy, University of Zagreb School of Medicine, Šalata 11, HR-10000 Zagreb, Croatia. E-mail: natasa.kovacic@mef.hr

doi: 10.1096/fj.201801426R

increase the expression of receptor activator of NF-κB ligand (RANKL) on osteoblastic and activated T cells and, thus, enhance osteoclastogenesis (12–14). Increased NF-κB signaling triggered by inflammatory cytokines also reduces the differentiation potential of mesenchymal cells in the affected joints (15–17). In addition, the inflammatory milieu suppresses the Wnt pathway, which is important for the differentiation and functioning of osteoblasts (18).

Pathogenesis of arthritis is also influenced by survival and apoptosis of inflammatory and synovial cells. Apoptosis can be induced externally, by the ligation of death receptors from the TNF family, which are able to activate caspase signaling *via* the intracytoplasmic death domain (19). Fas (CD95, Apo-1), a typical death receptor, is a well-characterized regulator of immune system homeostasis and is ubiquitously expressed on different cells and tissues (20). Increasing evidence suggests the involvement of the Fas/Fas ligand (FasL) system in bone homeostasis (21–25). The Fas/FasL system has already been implicated in the pathogenesis of RA and other inflammatory arthritides, but there are contradicting reports on its beneficial, as well as detrimental, roles in the pathogenic process (26, 27). For instance, hyperplastic FLS and infiltrating cells express Fas, so administration of the Fas-agonistic antibody or FasL delivery ameliorated arthritis (28–30). However, hyperplastic FLS are resistant to apoptosis because of the expression of the antiapoptotic molecules or the inadequate contribution of the internal, mitochondrial apoptotic pathway (31, 32). In contrast, systemic inactivation of Fas in the DBA/lpr mouse strain alleviates murine collagen-induced arthritis because of ineffective signaling through IL-1R in macrophages (33, 34). A recent study (35) also showed faster resolution of K/BxN murine arthritis, in mice with conditional depletion of Fas in their myeloid cells due to reduced expression of the TLR2 ligand gp96 and enhanced expression of IL-10 in the macrophages. In this study, we report on the attenuated form of antigen-induced arthritis (AIA) in Fas-deficient ($Fas^{-/-}$) mice and address the potential role of Fas in the regulation of local bone formation under arthritic conditions by controlling synovial bone and cartilage progenitor apoptosis and differentiation.

MATERIALS AND METHODS

Mice

Female C57BL/6 wild-type (WT) mice (8–12 wk old) and mice deficient in the Fas gene ($Fas^{-/-}$) on a C57BL/6 background (36) were used in all experiments. The $Fas^{-/-}$ mice strain and its corresponding WT controls (C57BL/6) were a gift from Dr. M. Simon (Max Planck Institute for Immunobiology, Freiburg, Germany). Both colonies were bred and maintained at the animal facility of the Croatian Institute for Brain Research, University of Zagreb School of Medicine (Zagreb, Croatia), under standard conditions [10/14-h light/dark daily, standard chow (4RR21/25; Mucedola, Milan, Italy) and water *ad libitum*]. All animal protocols were approved by the Ethics Committee of the University of Zagreb School of Medicine (380-59-10106-15-168/235) and the National Ethics Committee (EP 07-2/2015) and were conducted in accordance with accepted standards of ethical care and use of laboratory animals.

AIA

Mice were immunized with 200 μg methylated bovine serum albumin (mBSA; MilliporeSigma, Burlington, MA, USA) emulsified in 0.2 ml complete Freund's adjuvant (MilliporeSigma) injected subcutaneously into the flank skin (9); 7 d after the first injection, the mice were injected intradermally with 100 μg mBSA in 0.1 ml complete Freund's adjuvant at the base of the tail. Arthritis was induced on d 21 by intraarticular (i.a.) injection of 50 μg mBSA dissolved in 10 μl sterile PBS into both knees, under tribromoethanol (MilliporeSigma) anesthesia. Controls were injected intraarticularly with 10 μl of sterile PBS. Mice were euthanized on d 31 (d 10 after i.a. injection) by cervical dislocation under tribromoethanol anesthesia. After skin removal, transverse diameters of knee joints were measured 3 times for each knee by a caliper. Right knees were harvested for histologic assessment of arthritis, histomorphometry, or microcomputerized tomography (μCT), and left knees were harvested for flow cytometry, cell sorting, and osteoblastogenic cultures.

Histologic assessment of arthritis

Knee joints were dissected, released from soft tissues, and fixed in 4% formaldehyde at 4°C for 24 h. Fixed tissues were decalcified for 2 wk in 14% EDTA and 3% formalin, dehydrated in increasing ethanol concentrations, and embedded in paraffin. Next, 6 μm sections were cut with an SM 2000 R rotational microtome (Leica Microsystems, Wetzlar, Germany). Histologic assessment was performed on the frontal sections (6 μm) through the knee joint stained with Goldner-trichrome or toluidine blue. Histologic sections were scored semiquantitatively in a blinded fashion (by concealing labels and random assignment of numbers before scoring) for the following parameters of joint destruction: synovitis, joint-space exudate, cartilage degradation, and subchondral bone damage, on a 0–3-point scale (37). A combined arthritis score was generated as the sum of scores for the above 4 parameters (maximum score, 12).

Histomorphometry

Histomorphometry was performed in a blinded fashion with an Axio Imager microscope (Carl Zeiss GmbH, Oberkochen, Germany) equipped with a charge-coupled device camera connected to a computer with appropriate software (OsteoMeasure; OsteoMetrics, Decatur, GA, USA).

Histomorphometric analysis was performed under ×100 magnification, in 4 Goldner-trichrome-, and toluidine blue–stained distal frontal femoral sections, taken from corresponding depths for each specimen, measuring mineralized trabeculae separately in the distal midepiphyseal region. Analyzed variables were automatically calculated by the OsteoMeasure software and included bone volume/total volume (BV/TV; %), trabecular number (Tb.N; per mm), trabecular thickness (Tb.Th; μm), and trabecular separation (Tb.Sp; mm).

μCT analysis

The distal femora were scanned with a μCT system (1076 SkyScan; Bruker microCT, Kontich, Belgium), at 50 kV and 200 μA with a 0.5 aluminum filter. Detection pixel size was

9 μm, and images were captured every 0.4° through 180° rotation of the camera. The scanned images were reconstructed with the Recon software (SkyScan; Bruker microCT) and analyzed using the CTAn software (SkyScan; Bruker microCT). Three-dimensional analysis and reconstruction of the epiphyseal trabecular bone was performed on transverse sections in the region beginning above the epiphyseal line (excluding the dense zones adjacent to the epiphyseal cartilage) and ending at the level of the separation of the condyles. Measured variables were BV/TV (%), Tb.N (per mm) Tb.Th (μm), and Tb.Sp (mm).

Flow cytometry and cell sorting

Tibiae and femora were cut at the level of the growth plates, and the isolated joints were cleaned from the surrounding soft tissues, injected with 1 mg/ml collagenase type IV (MilliporeSigma), and incubated for 1 h at 37°C to release the synovial cells. Cultured synovial cells were dissociated from the surface with TrypLE Express (Thermo Fisher Scientific, Waltham, MA, USA). Single-cell suspensions were prepared by passing the cells through a 100-μm cell strainer, and suspensions containing 2–5 $\times$ 10^6 cells were transferred to FACS tubes. Nonspecific antibody binding was blocked by adding 0.5 μl/sample of anti-mouse CD16/CD32 (93; Thermo Fisher Scientific) and incubating for 5 min at room temperature. After blocking, cells were stained with 6-color panels and the following antibodies: anti-CD95-AF488 (15A7; Thermo Fisher Scientific) and/or anti-CD95-FITC (Jo2; BD Biosciences, San Jose, CA, USA) or the corresponding isotype controls (mouse IgG1κ-AF488; Thermo Fisher Scientific; and Armenian hamster IgG2λ-FITC; BD Biosciences), CD45-allophycocyanin (APC; 30-F11; Thermo Fisher Scientific), CD31-phycoerythrin cyanine 7 (PECy7) or APC (390; Thermo Fisher Scientific), TER119-PE or APC (TER119; Thermo Fisher Scientific), CD51-biotin (RMV-7; BioLegend, San Diego, CA, USA), CD200-PE (OX90; Thermo Fisher Scientific), CD105-PECy7 (MJ7/18; Thermo Fisher Scientific), CD90.2-FITC (30-H12; Thermo Fisher Scientific), Sca-1-FITC (D7; Thermo Fisher Scientific), CD140b-PECy7 (APB5; Thermo Fisher Scientific), CD11b-PE (M1/70; Thermo Fisher Scientific), Gr-1-PECy7 (RB6-8C5; Thermo Fisher Scientific), B220-APC (RA3-6B2; Thermo Fisher Scientific), and CD3-APCCy7 (145-2C11; Thermo Fisher Scientific). Dead cells were excluded by binding of 7-amino-actinomycin D (7-AAD; BioLegend) or propidium iodide (PI; Thermo Fisher Scientific). After incubation for 30 min at 4°C, cells were washed with PBS and incubated with streptavidin-APCeFluor780 (Thermo Fisher Scientific) for 30 min at 4°C, washed, resuspended in PBS containing 10 μl of 7-AAD/ml, acquired on an Attune (Thermo Fisher Scientific) instrument and analyzed by FlowJo software (FlowJo, Ashland, OR, USA). Annexin V (BioLegend) and 7-AAD staining were performed according to the manufacturer's instructions.

Cell sorting was performed with a BD FACSAria I (BD, Franklin Lakes, NJ, USA) instrument, as previously described (38). Labeled cells were acquired at a speed 2000–5000 cells/s with the following gating strategy: singlets were delineated from total cell population depicted on forward- *vs.* side-scatter plots, and exclusion of dead cells was based on DAPI dihydrochloride (MilliporeSigma) incorporation and subsequent dissection of populations of interest. Defined populations of hematopoietic and stromal cells were sorted in 2-ml collection tubes containing PBS with 2% fetal calf serum and used for cell cultures. Sorting parameters were optimized for high-purity sorting. Sorting purity was determined by a reanalysis of fractioned populations and was >99% for all experiments.

Cell culture

Cells were plated in 6- or 24-well culture plates at a density of 2.5 $\times$ 10^5 cells in 0.35 ml of α-minimum essential medium/cm^2 surface for primary cultures, and 1.5 $\times$ 10^4 cells in 0.35 ml of α-minimum essential medium/cm^2 surface for sorted mesenchymal cell cultures, supplemented with 10% fetal calf serum (Thermo Fisher Scientific). Osteoblast differentiation was induced with the addition of 50 μg/ml ascorbic acid, 10^{-8} M dexamethasone, and 8 mM β-glycerophosphate. Osteoblast colonies were identified histochemically by the activity of alkaline phosphatase (AP) with a commercially available kit (MilliporeSigma). Red-stained AP^+ osteoblast surface/well was measured with custom-made software (39). Mineralization was estimated by alizarin red (MilliporeSigma) staining and semiquantified by acetic acid–mediated extraction of dye and spectrophotometry (40). Total colonies were stained with methylene blue (MB).

Induction of apoptosis

For the induction of apoptosis, 1 μg/ml of anti-mouse CD95 antibody (clone Jo2; BD Biosciences) or the corresponding isotype control (Armenian hamster IgG2λ; BD Biosciences) and 1 μg/ml protein G (MilliporeSigma) were added to osteoblastogenic cultures on d 6 and 13 and incubated for 16–18 h. Cells treated with only 1 μg/ml protein G were used as nontreated controls.

Gene expression analysis

Total RNA was extracted using a Trizol reagent (Thermo Fisher Scientific). For PCR amplification, total RNA was converted to cDNA by reverse transcriptase (Thermo Fisher Scientific), and amplified with an ABI 7500 instrument (Thermo Fisher Scientific) with commercially available TaqMan Assays (mouse Fas, Mm00487425_m1; mouse FasL, Mm00438864_m1; mouse TNF, Mm00443258_m1; mouse IL1-β, Mm00434228_m1; mouse RANKL, Mm00441906_m1; mouse osteoprotegerin (OPG), Mm00435452_m1; mouse IL-6, Mm00446190_m1; mouse IL-10, Mm01288386_m1; mouse β-actin, Mm00607939_s1; mouse Runx2, Mm00501584_m1; mouse Col1a2, Mm00483888190_m1; and mouse osteocalcin, Mm03413826_mH; Thermo Fisher Scientific), as previously described (21).

Data analysis and interpretation

Data are plotted as individual values, with horizontal lines and markers representing means ± SD, or medians ± interquartile range (IQR). Statistical analysis has been performed by MedCalc Statistical Software v.12.5.0 (MedCalc Software bvba, Ostend, Belgium). Depending on the number of factors, distribution, and type of variables, data were analyzed by 2- or 1-way ANOVA with Student-Newman-Keuls *post hoc* test, or Kruskal-Wallis test with pairwise comparisons according to Conover (41).

RESULTS

Functional Fas receptor is required for development of destructive AIA

To assess the effects of Fas inactivation on the severity of AIA, we first analyzed joint swelling, histologic signs of joint destruction, and characteristics of epiphyseal bone (**Fig. 1*A***). Ten days after i.a. injection, the transverse

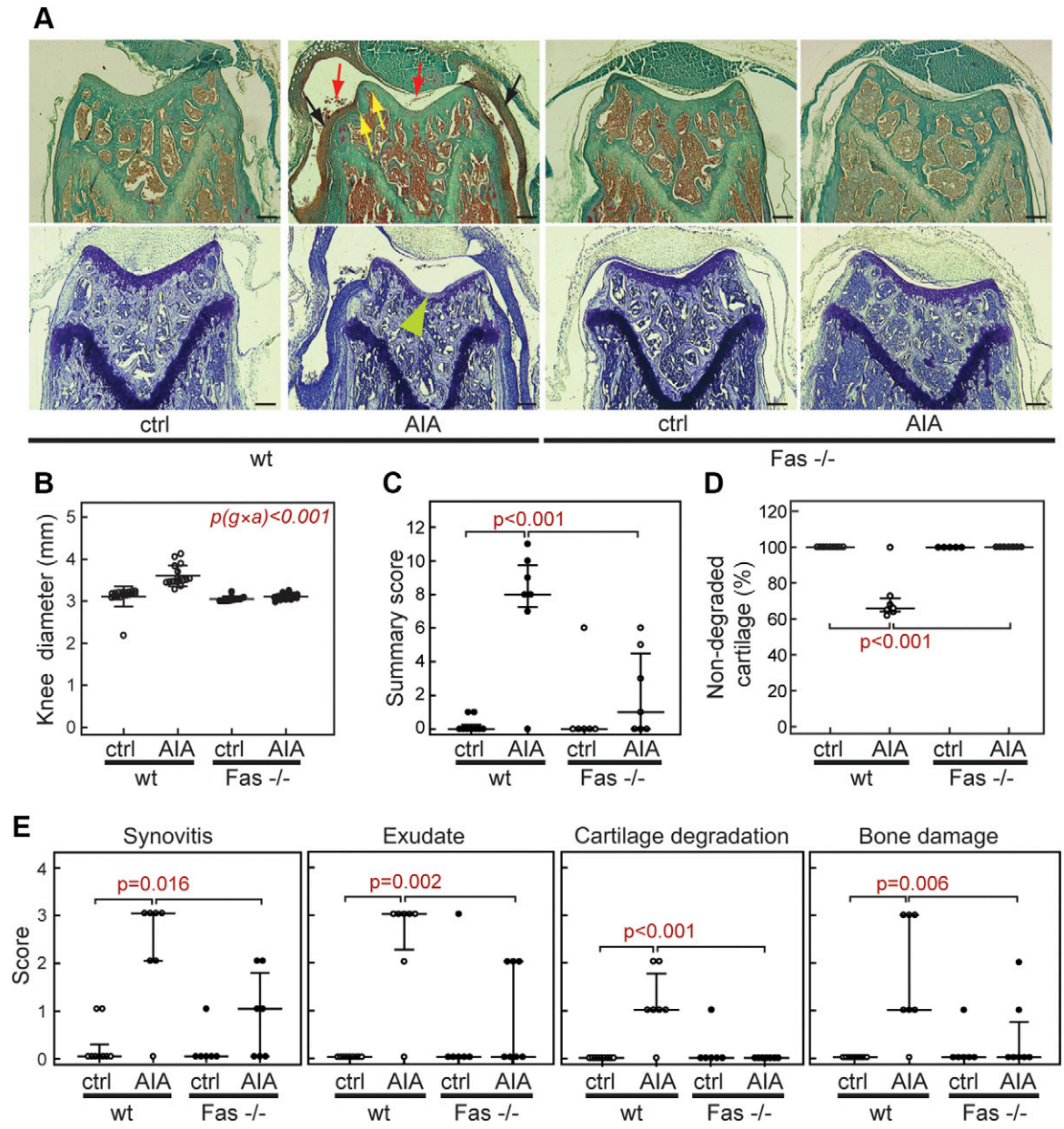

Figure 1. Arthritis score in WT and Fas$^{-/-}$ mice. The WT and Fas$^{-/-}$ mice were sacrificed on d 10 after i.a. injection of mBSA. *A*) Representative images of 6-μm Goldner-trichrome (top) and toluidine-blue (bottom row)–stained midfrontal femoral sections of WT and Fas$^{-/-}$ mice, intraarticularly injected with mBSA (AIA) or PBS [control (ctrl)]. Histology scoring was performed in a blinded fashion according to synovial thickening (black arrows), exudate in joint space (red arrow), cartilage degradation (green arrowhead), and subchondral bone damage (yellow arrows), according to the 3 point scale. *B*) Transverse diameter of both knees was measured after sacrifice and skin removal with a caliper. *C*) Total histology score was measured in the right knee of WT and Fas$^{-/-}$ mice intraarticularly injected with mBSA (AIA) or PBS (ctrl). *D*) Percentage of nondegraded cartilage thickness of the total cartilage thickness in WT and Fas$^{-/-}$ mice intraarticularly injected with mBSA (AIA) or PBS (ctrl), measured by histomorphometry. *E*) Separate histology scores in WT and Fas$^{-/-}$ mice intraarticularly injected with mBSA (AIA) or PBS (ctrl). Data are from one representative of 3 repeated experiments, in which both knees were measured 3 times and the mean values for each knee were used for statistical analysis (B6 ctrl, n = 18; B6 AIA, n =16; Fas ctrl, n = 12; and Fas AIA, n = 14). Right knee was used for histology scoring and cartilage thickness measurements (B6 ctrl, n = 9; B6 AIA, n = 7; Fas ctrl, n = 6; and Fas AIA, n = 7, excluding 1 slide in the B6 AIA group because of inappropriate orientation). Markers represent individual values. Horizontal lines and error bars are means ± SD (*B*) or medians ± IQR (*C–E*). The influence of genotype (g) and arthritis (a) on knee diameter was assessed by 2-way ANOVA, and statistical significance of the interaction between both factors, $p(g \times a)$ is marked on the plot (*B*). Kruskal-Wallis test (*C–E*); scale bars, 150 μm.

diameters of knee joints were greater in WT mice with AIA than they were in the WT control group (Fig. 1*B*), and such an increase was absent in Fas$^{-/-}$ mice (Fig. 1*B*). The summary histology score was significantly higher in WT mice with arthritis, in comparison to respective control (Fig. 1*C*). Analysis of individual scored elements showed that mild synovitis and exudate occasionally developed in arthritic Fas$^{-/-}$ mice, whereas bone and cartilage destruction

were even less common, in contrast to arthritic WT mice (Fig. 1*E*). A superficial zone of degraded cartilage was a common finding in WT mice with arthritis but was extremely rare in any of the other groups. Quantitatively assessed, the percentage of nondegraded cartilage in the total cartilage thickness was significantly less in WT mice with arthritis (Fig. 1*D*). In Fas$^{-/-}$ mice, both in the control group and in mice with arthritis, we observed only nondegraded cartilage (Fig. 1*D*).

Assessed by both histomorphometry and μCT, distal femoral epiphyseal trabecular bone volume and Tb.Th responded differently to arthritis in Fas$^{-/-}$ mice than they did in WT controls. Both variables were decreased in WT mice with AIA in comparison to the control group and were similar in both groups of Fas$^{-/-}$ mice (**Fig. 2*A*, *C***). μCT analysis showed irregularities and multiple erosions on the epiphyseal subchondral bone plate in WT AIA, which were absent in Fas$^{-/-}$ mice (Fig. 2*B*). In addition,

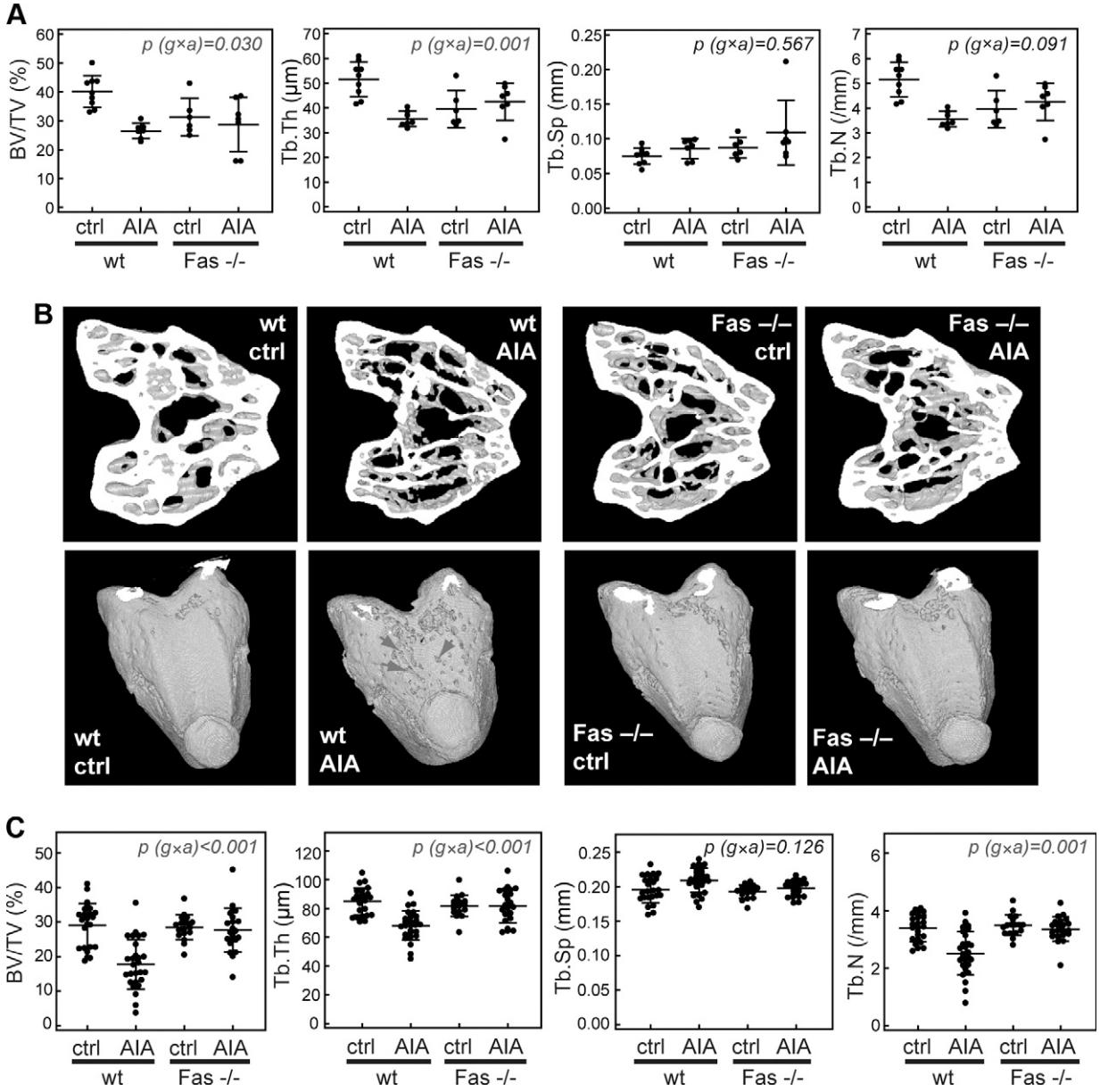

Figure 2. Histomorphometry and μCT analysis of distal femoral epiphyseal trabecular bone of WT and Fas$^{-/-}$ mice on d 10 of AIA. The following variables were analyzed in distal femoral epiphyses from WT and Fas$^{-/-}$ mice intraarticularly injected with mBSA (AIA) or PBS [control (ctrl)]: BV/TV (%), Tb.N (per mm), Tb.Th (μm), and Tb.Sp (mm). Histomorphometry analysis of the trabecular bone in the distal femoral epiphyses (*A*), representative 3-dimensional models of distal femora, from μCT reconstruction images (*B*), and quantitative μCT analysis of the trabecular bone in the distal femoral epiphyses (*C*). Histomorphometry data are from one representative of 3 repeated experiments (B6 ctrl, $n = 9$; B6 AIA, $n = 7$; Fas ctrl, $n = 6$; and Fas AIA, $n = 7$), and μCT are cumulative data from 3 representative experiments (B6 ctrl, $n = 24$; B6 AIA, $n = 27$; Fas ctrl, $n = 18$; and Fas AIA, $n = 22$). Markers represent individual values. Horizontal lines and error bars are means ± SD. Influence of genotype (*g*) and arthritis (*a*) on each bone-related variable was assessed by 2-way ANOVA, and statistical significance of interaction between both factors, $p(g \times a)$ is marked on plots. Arrows, bone erosions.

μCT revealed a different response of Tb.N in $Fas^{-/-}$ mice with arthritis, characterized by lower Tb.N in WT mice with AIA and similar in $Fas^{-/-}$ mice with AIA, in comparison to their respective controls (Fig. 2*C*).

Fas expression is up-regulated in AIA in hematopoietic and nonhematopoietic cells

To determine the populations potentially regulated by Fas in AIA, we analyzed the surface expression of Fas on hematopoietic ($CD45^+TER119^+$) and endothelial ($CD31^+$) *vs.* nonhematopoietic ($CD45^-TER119^-CD31^-$) cells in the joints from mice with arthritis and control mice. We expected that immunization itself would affect the expression of Fas because of the activation of cells of the immune system, so we also analyzed cells from the nonimmunized (NI) mice in addition to the immunized (IM) control and arthritic mice to distinguish the effect of immunization from the effect of local inflammation after arthritis induction. The systemic effect was further assessed by analyzing Fas expression on the splenocyte subsets in all 3 experimental groups.

Flow cytometry analysis showed a significant increase in the surface expression of Fas on the total population of synovia-derived cells in control immunized mice groups, in comparison with the control NI group. In mice with arthritis, expression was less than it was in control immunized mice but still significantly more than in the control NI group (**Fig. 3*A***, top left). The same pattern of expression was observed on the hematopoietic and nonhematopoietic populations (Fig. 3*A*, top). The pattern of expression of separately analyzed hematopoietic CD45, CD31, and TER119 synovia-derived populations was similar (Fig. 3*A*, middle). On the systemic level, assessed by analyzing

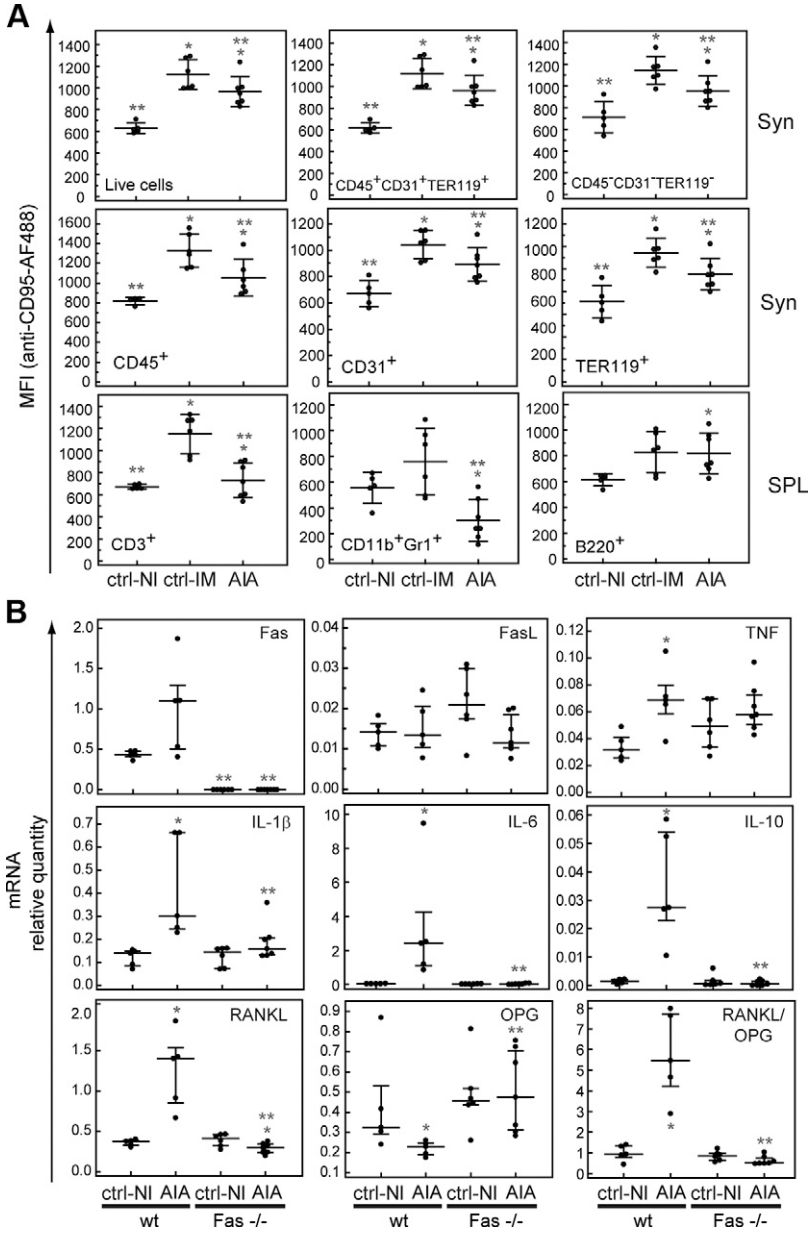

Figure 3. Expression of Fas on hematopoietic and nonhematopoietic lineage cells on d 10 of AIA. *A*) Cells from the synovial compartment (Syn) and spleen (SPL) from control NI mice (ctrl-NI), immunized mice injected intraarticularly with PBS (ctrl-IM) and with mBSA (AIA) were harvested, and synovial single-cell suspensions were stained with anti-mouse CD95-AF488 or the corresponding isotype control, anti-mouse CD45-APC, TER119-PE, and CD31-PECy7 antibodies, whereas spleen cells were stained with anti–CD95-AF488 or the corresponding isotype control, CD11b-PE, Gr-1-PECy7, B220-APC, and CD3-APCCy7 antibodies. Data are from one representative of 2 repeated experiments. Both knees from each mouse were harvested and pooled for flow cytometry analysis, which was performed separately for each mouse (ctrl-NI, $n = 5$; ctrl-IM, $n = 6$; and AIA, $n = 7$). Mean fluorescence intensities for each population are shown as individual values (markers). Horizontal lines and bars are means ± SD. $^*P < 0.05$ *vs.* ctrl-NI mice, $^{**}P < 0.05$ *vs.* ctrl-IM mice, by ANOVA and Student-Newman-Keuls *post hoc* test. *B*) Expression of Fas, FasL, TNF, IL-1β, IL-6, IL-10, RANKL, and OPG mRNA in total knee joint tissue from ctrl-NI, immunized WT, and $Fas^{-/-}$ mice injected intraarticularly with mBSA (AIA). Both knees from each mouse were harvested and pooled for RNA extraction (WT ctrl-NI, $n = 5$; WT AIA, $n = 5$; $Fas^{-/-}$ ctrl-NI, $n = 6$; and $Fas^{-/-}$ AIA, $n = 7$). Markers represent gene expression values of an individual mouse, normalized to gene expression of β actin. Horizontal lines and error bars are medians ± IQR. $^*P < 0.05$ *vs.* ctrl-NI mice, $^{**}P < 0.05$ *vs.* WT mice, by the Kruskal-Wallis test.

splenocyte subsets, the expression pattern on T cells was similar to synovia-derived populations and was characterized by increased expression of Fas because of immunization, and a decrease in Fas upon induction of arthritis. Expression of Fas on myeloid ($CD11b^+Gr1^+$) splenocyte population was not different between immunized and NI controls and was down-regulated in mice with arthritis. Expression of Fas on splenic B cells was similar in both immunized groups and was slightly greater than in the NI mice (Fig. 3*A*, bottom). Taken together, this reveals that both immune and osteoprogenitor populations are potential cellular targets of the Fas/FasL system in arthritis.

To assess the overall regulation of Fas/FasL system, in the context of inflammatory activity and bone remodeling, we analyzed the expression of selected genes in total joint tissue extracts from WT and $Fas^{-/-}$ mice with arthritis, and compared them with baseline expression in NI mice. On d 10 after induction of arthritis, Fas expression was more than 2-fold up-regulated in only 3 of 5 samples from WT mice in comparison to NI controls, so the overall increase was not significant (Fig. 3*B*, top). This was potentially a result of assessment at d 10, when inflammatory activity was ceasing. In early acute arthritis (d 3 after induction), we detected a 2–5-fold increase in all samples of WT mice with arthritis in comparison with NI controls ($P = 0.005$, $n = 4$, Kruskal-Wallis test, data not shown), pointing to transcriptional up-regulation in early arthritis. The expression of FasL was similar in all groups of mice (Fig. 3*B*, top). Major proinflammatory cytokines TNF, IL-1β, and IL-6 (Fig. 3*B*, top right and middle) were, as expected, greater in WT mice with arthritis than in NI WT mice. The levels of IL-1β and IL-6, as well as that of anti-inflammatory IL-10 were also significantly greater in WT mice with AIA in comparison with $Fas^{-/-}$ mice with AIA, whereas levels of TNF were comparable between both groups of mice with arthritis. This overall cytokine profile points to a conclusion that inflammation was less extensive in the joints of $Fas^{-/-}$ mice with AIA, which is further in line with the results of histology scoring, but contrasts with the previously described findings in *lpr* mice with collagen-induced arthritis (33). Absence of bone loss in $Fas^{-/-}$ mice was reflected in the expression of RANKL and OPG as important regulators of bone remodeling. Joints from WT mice with arthritis expressed significantly more pro-osteoclastogenic RANKL than NI WT mice, whereas the levels were lower in $Fas^{-/-}$ mice with arthritis in comparison with their NI controls, as well as in comparison with the WT AIA group. At the same time, expression of anti-osteoclastogenic OPG was decreased in WT mice with AIA in comparison with NI control and $Fas^{-/-}$ mice with AIA and was similar in both $Fas^{-/-}$ groups (Fig. 3*B*, bottom). The RANKL/OPG ratio was thus increased in WT mice with AIA, similar in both groups of $Fas^{-/-}$ mice, and significantly less in $Fas^{-/-}$ mice with AIA in comparison with the WT AIA group, confirming the bone-preserving effect of Fas deficiency in the subacute phase of AIA documented by histology and histomorphometry (Fig. 3*B*, bottom right).

Synovial subpopulations of bone and cartilage progenitors are differentially regulated in Fas-deficient mice with arthritis

Up-regulation of Fas in arthritis, and alterations in inflammatory cytokine expression, point to a role for Fas in the regulation of many aspects of joint inflammation, which could directly or indirectly induce misbalanced bone remodeling and result in permanent joint damage. Suppressed inflammation and a decreased RANKL/OPG ratio in $Fas^{-/-}$ mice with arthritis point toward Fas being required to support inflammation and enhance osteoclastogenesis. However, as we previously described for the effects of Fas on osteoblast maturation and apoptosis (21), we hypothesized that bone-sparing effect of Fas inactivation might also be mediated through non-hematopoietic population containing bone and cartilage progenitors. In addition to its role in reparative processes, this population is also the source of OPG, whose expression was altered by Fas deficiency.

We first assessed osteoblast differentiation from total synovial cells. Cells were harvested on d 10 after i.a. injection, and the surface covered with AP positive colonies was measured after 14 d of cell culture. To confirm osteoblastogenic differentiation, we determined the expression of early osteoblast-specific genes, runt-related transcription factor 2 (*Runx2*) and collagen type I, α2 chain (*Col1α2*), and mature osteoblast-specific genes, osteocalcin (*bglap*) and osteoprotegerin (*OPG*), over the culture course. Osteoblastogenesis was not significantly different among groups of mice, which was reflected by lack of significant effect of Fas deficiency or arthritis on the surface covered by AP^+ osteoblast colonies as well as on the expression of osteoblast genes (**Fig. 4*A–C***). *Ex vivo* culture conditions reflected the number and differentiation potential of mesenchymal cells, but not necessarily their differentiation within the inflammatory microenvironment, so we further focused on the analysis of proportions of resident subpopulations of nonhematopoietic synovial cells ($CD45^-TER119^-CD31^-$), and among them, proportions of cells bearing various mesenchymal and osteoblast markers, such as Sca-1, CD140b, and CD44, and a modified set of osteoprogenitor markers recently characterized by Chan *et al.* (42). According to Chan *et al.* (42), osteoprogenitors are contained among the population of $CD51^+CD45^-TER119^-CD31^-$ cells and were further separated according to the expression of CD200, CD90.2, and CD105. $CD51^+CD200^+$ cells correspond to the earliest progenitors [skeletal stem cells (SSCs)], whereas $CD51^+CD200^-$ cells were committed progenitors (Fig. 4*D*). Further osteogenic/chondrogenic differentiation resulted in acquisition of CD105 and CD90.2 markers. Committed cartilage progenitors coexpress CD200 and CD105, so we considered $CD200^+CD105^-$ to be SSCs. The proportion of the total nonhematopoietic $CD51^+CD45^-TER119^-CD31^-$ population was not affected by arthritis or Fas inactivation (Fig. 4*E*), and the proportions of $CD140b^+$, $Sca\text{-}1^+$, and $CD44^+$ cells had no consistent pattern among experiments (data not shown). In WT mice with arthritis, the proportion of $CD51^+CD200^+$ cells (SSCs) was lower in comparison to control mice and was accompanied by a

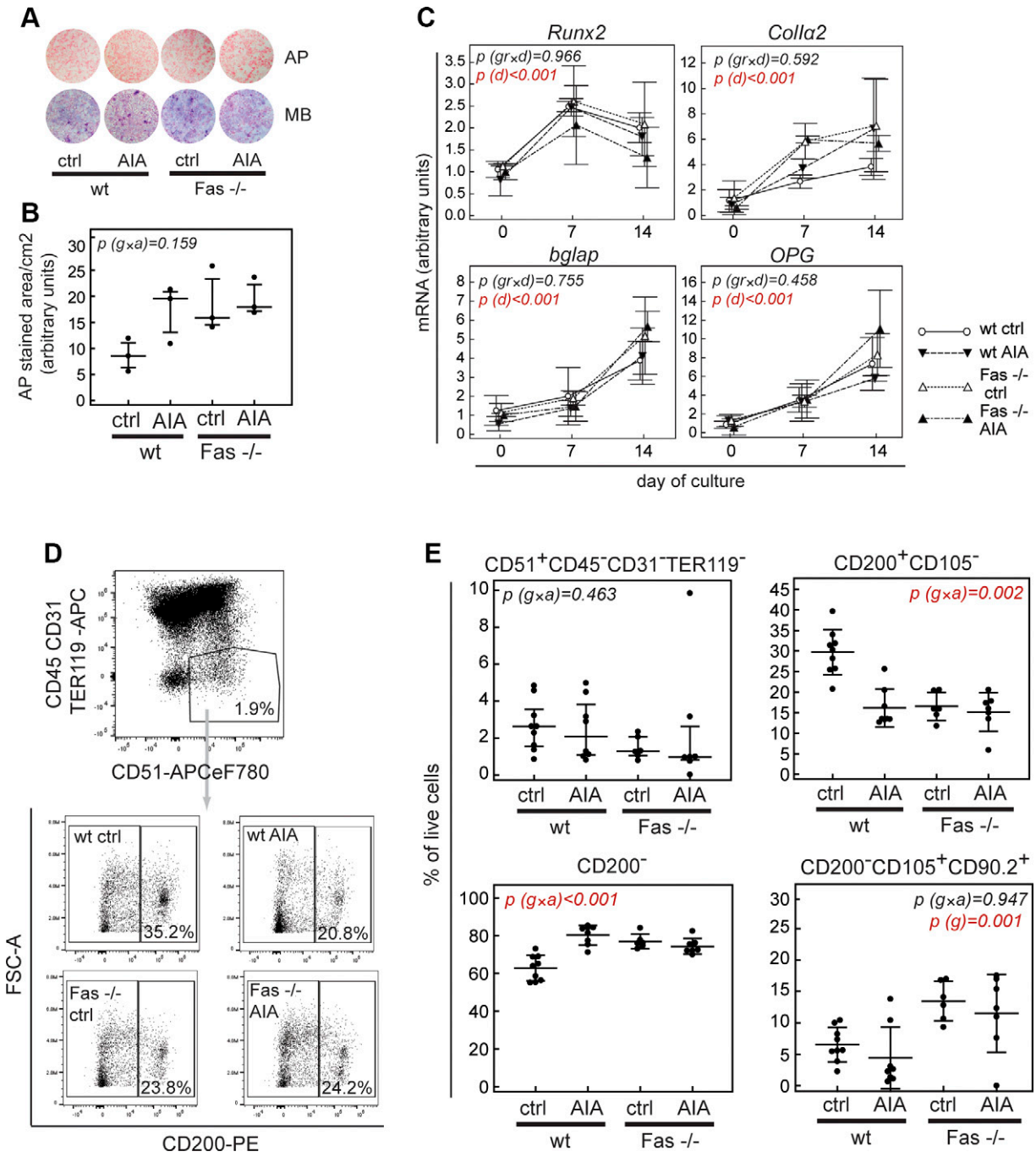

Figure 4. Osteoblastogenesis and proportions of synovial nonhematopoietic cells in WT and Fas$^{-/-}$ mice with AIA. *A*) Synovia-derived osteoblast colonies from immunized WT and Fas$^{-/-}$ mice injected intraarticularly with PBS [control (ctrl)] and mBSA (AIA) on d 14 of cell culture, stained for AP (red) and with MB. Data are from 1 of 3 repeated experiments, in which cells were isolated from 6–8 mice/group and pooled for culture. *B*) Semiquantitative data are means ± SD of AP$^+$ surface/square centimeter-triplicate wells of a 6-well culture plate (n = 3). Influence of genotype (g) and arthritis (a) on AP$^+$ surface was assessed by 2-way ANOVA. Statistical significance of the interaction between both factors, $p(g \times a)$ is marked on the plot. *C*) Expression of osteoblast genes *Runx2* and *Collα2*, osteocalcin (*bglap*), and osteoprotegerin (*OPG*) during synovia-derived osteoblast differentiation. The data are from 2 repeated experiments in which cells were isolated from 6–8 mice/group and pooled for culture. RNA was harvested from 3 pooled wells of a 24-well culture plate. Relative quantity of a gene in each experiment was normalized to the relative quantity of β actin and the average quantity of each gene on a culture d 0. Horizontal lines and bars are means ± SD of both experiments (n = 2). Influence of experimental group (gr) and culture day (d) on expression of each gene was assessed by 2-way ANOVA. Statistical significance of the interaction between both factors, $p(gr \times d)$, and significant influence of culture day, $p(d)$ is marked on the plots. For flow cytometry analysis, single-cell suspensions were stained with anti-mouse CD90.2-FITC, CD200-PE, CD105-PECy7, CD45-APC, TER119-APC, CD31-APC, and CD51-biotin/streptavidin-APCeF780 antibodies. Dead cells were excluded by binding of 7-AAD. Proportions of CD45$^-$TER119$^-$CD31$^-$CD51$^+$ (nonhematopoietic bone and cartilage progenitor) cells were determined among single, live cells. Proportions of CD200$^+$CD105$^-$, CD200$^-$, and CD200$^-$CD105$^+$CD90.2$^+$ cells were determined among CD45$^-$TER119$^-$CD31$^-$CD51$^+$

(*continued on next page*)

corresponding increase in the proportion of $CD51^+CD200^-$ cells, whereas the ratio between both populations was similar in control and AIA groups of $Fas^{-/-}$ mice (Fig. 4*E*). The frequency of cells corresponding to committed bone progenitors ($CD51^+CD200^-CD105^+CD90.2^+$) was not altered by arthritis, but higher frequencies were observed in $Fas^{-/-}$ mice, pointing to changed differentiation kinetics in Fas deficiency (Fig. 4*E*).

Synovial bone and cartilage progenitors express Fas and have a different susceptibility to Fas-mediated apoptosis

To confirm the functional role of Fas receptor on synovia-derived bone and cartilage progenitors, we assessed the expression and function of Fas during osteoblastogenic differentiation of mesenchymal progenitors from the synovial compartment. To establish pure, primary mesenchymal population, we used fluorescence-activated cell sorting of $CD45^-CD31^-TER19^-CD51^+$ cells and expanded them *in vitro*. Flow cytometry analysis confirmed the absence of hematopoietic or endothelial markers, high expression of CD51, substantial expression of CD200, and variable expression of CD105 (**Fig. 5*A*, *B***). Osteoblast differentiation *in vitro* was marked by an increase in proportion of $CD200^+$ cells and a corresponding decrease in $CD200^-$ cells (Fig. 5*A*, *B*). In osteoblastogenic cultures, 80–90% cells expressed Fas on a culture d 7, with a decrease to 50–70% toward d 14 and corresponding results on the transcriptional level (Fig. 5*C*–*E*). Expression of Fas was less on $CD200^-$ cells, with a prominent decrease toward d 14 in comparison to $CD200^+$ cells (Fig. 5*C*, *D*). Synovial progenitors were capable of forming AP^+ colonies on both d 7 and 14 and later in the culture course (d 14) alizarin red-stained, mineralized nodules (Fig. 5*F*, *G*).

To establish the function of Fas receptor expressed on mesenchymal progenitors, we treated those cultures with anti-Fas antibody on d 6 and 13, which resulted in a substantial increase in the numbers of apoptotic and dead cells on d 7 and 14 (**Fig. 6*A***); 16 h after Fas treatment, there was a reduction in proportion of $CD200^+$ cells at both time points in the osteoblastogenic cultures (Fig. 6*B*), confirming that $CD200^+$ cells are susceptible to Fas-induced apoptosis.

DISCUSSION

This study reveals an important role of the Fas receptor in the development of the destructive form of murine AIA, not only by supporting inflammation but also by inducing osteoprogenitor apoptosis and thus, affecting bone formation. Clinical and histologic scoring showed a particular absence of cartilage and bone destruction in Fas-deficient mice with AIA, with mild inflammation occasionally present. In addition to the absence of subchondral bone erosions, the loss of epiphyseal trabecular bone and the thinning of the epiphyseal trabeculae were absent in $Fas^{-/-}$ mice, in comparison to the WT mice with arthritis, which is in accordance with our previous findings on the positive effects of the Fas/FasL system deficiency on bone mass (23, 43). In this report, we quantified the subchondral epiphyseal trabecular bone to assess the bone damage associated specifically with local inflammation, rather than the standard quantification of metaphyseal bone, which might also reflect the existence of systemic inflammation-induced osteopenia.

Our findings are consistent with previous studies documenting attenuated murine collagen-induced arthritis and faster resolution of the chronic phase of K/BxN arthritis in murine models of Fas inactivation (33–35). These results were ascribed to altered proinflammatory signaling through IL-1R and revealed Fas signaling in macrophages as an important regulator of the inflammatory process (33–35). In contrast to these studies, which report similar or increased levels of proinflammatory cytokines in joints of Fas-deficient mice in comparison to controls on protein or transcriptional levels, we found decreased levels of major proinflammatory cytokines IL-1β and IL-6 in $Fas^{-/-}$ mice with AIA. This might reflect the different experimental models of arthritis or the mouse strain used in the above-mentioned studies. *lpr* mice used in studies by Tu-Rapp *et al.* (33), and Ma *et al.* (34) are described as having leaky spontaneous mutation, which may account for differences in the pathogenic mechanism (36). In addition, these discrepancies could be time related. A detailed kinetic study of cytokine expression performed in rats revealed differences in cytokine expression over the course antigen-induced arthritis. TNF transcription peaks during first 24 h after i.a. injection of antigen, and after that, it returns to basal levels, whereas IL-1β, and in particular IL-6, retain transcriptional elevation for 2 wk (44). Therefore, our results on d 10 after induction do not fully depict the complex changes of cytokine pattern over the disease course but provide additional evidence for less-extensive inflammation at that time point, already established by histology score. However, the crucial outcome assessed in our study was local bone damage, which results in deformities and disability and represents clinically important features of RA, developing because of the complex interactions between immune cells, as well as resident cell populations in the affected joints. Certain forms of autoimmune and inflammatory arthritides, such as the arthritis

cells. *D*) Dot plots show $CD200^+$ and $CD200^-$ cells in the concatenated samples from a representative experiment. *E*) Top: proportions of $CD45^-TER119^-CD31^-CD51^+$ cells in total live synovial cells. Bottom: $CD200^+CD105^-$, $CD200^-$, and $CD200^-CD105^+CD90.2^+$ in $CD45^-TER119^-CD31^-CD51^+$cells, shown as individual values (markers). Data are from one representative of 3 repeated experiments, in which left knees were used for cell dissociation and flow cytometry. Horizontal lines and bars are means ± SD (B6 ctrl, $n = 9$; B6 AIA, $n = 8$; Fas ctrl, $n = 6$; and Fas AIA, $n = 7$). Influence of genotype (g) and arthritis (a) on proportions of osteoprogenitor populations was assessed by 2-way ANOVA. Statistical significance of interaction between both factors, $p(g \times a)$, and significant influence of genotype, $p(g)$, are marked on the plots.

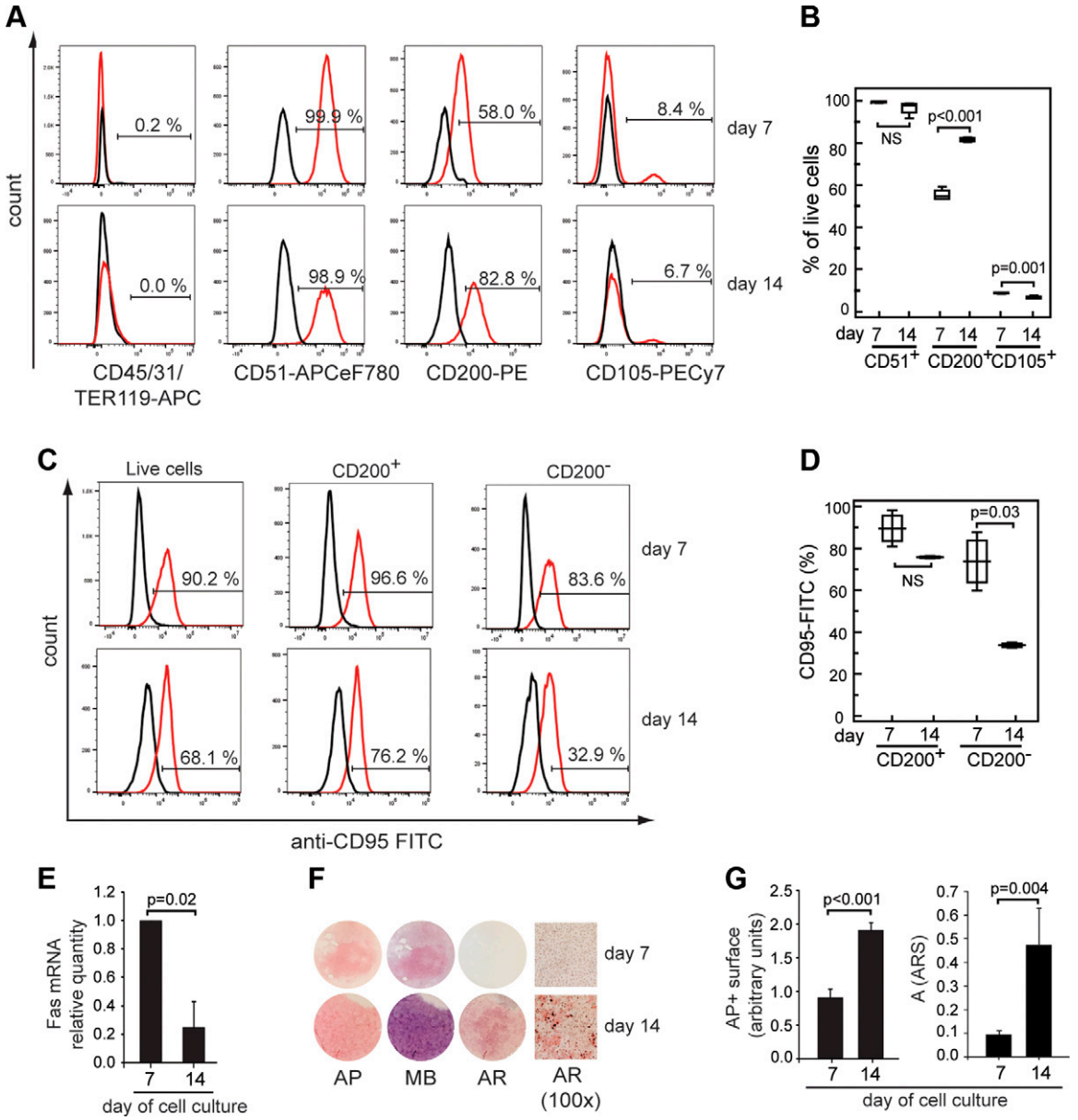

Figure 5. Expression of Fas in synovial mesenchymal cells. *A*) Representative histograms (red histograms, stained cells; black histograms, nonstained cells) on d 7 (top row) and d 14 (bottom row), and *B*) proportions of live cells expressing hematopoietic and mesenchymal markers in osteoblastogenic cultures of sorted $CD45^-CD31^-TER119^-CD51^+$ cells. Cultured cells were harvested on culture d 7 and 14 and were labeled with anti-mouse CD95-FITC or the isotype control, anti-mouse CD45-APC, CD31-APC, TER119-APC, CD51-APCeF780, CD200-PE, and CD105-PECy7. Experiments were repeated 3 times, and data are means of quadruplicate wells of the representative experiment. Statistical significance is marked on plots (d 7 *vs.* 14, by *t* test). *C*) Representative histograms on culture d 7 (top row) and d 14 (bottom row). Cultured cells were labeled with anti-mouse CD95-FITC, and the proportion of $CD95^+$ cells (red histograms) was determined according to the signal of corresponding isotype control (black histograms). *D*) Proportions of live $CD200^+$ and $CD200^-$ cells labeled with anti-mouse CD95-FITC, in osteoblastogenic cultures of sorted $CD45^-CD31^-TER119^-CD51^+$ cells. Experiments were repeated 3 times, and data are means of duplicate wells of the representative experiment. Statistical significance is marked on the plots (d 7 *vs.* 14, by Student's *t* test). *E*) Expression of Fas mRNA in osteoblastogenic cultures of sorted mesenchymal progenitors ($CD45^-CD31^-TER119^-CD51^+$). Data are means ± SD of Fas mRNA relative expression in 3 repeated experiments ($n = 3$), normalized to quantity on a d 7; statistical significance is marked on the plot (d 7 *vs.* 14, by *t* test). *F*) Osteoblast cultures from sorted mesenchymal progenitors ($CD45^-CD31^-TER119^-CD51^+$) on d 7 and 14 of cell culture, stained for AP, with alizarin red (AR), and total colonies stained with MB. Mineralized nodules are also shown in the microphotograph (AR; magnification, ×100). *G*) Semiquantitative assessment of AP^+ red surface area, and absorbance (A) of acetic acid–extracted AR on d 7 and 14 of cell culture, both measured in 4 wells of 6-well culture plate. Data are means ± SD of 4 replicates ($n = 4$). Statistical significance is marked on the plot (d 7 *vs.* 14, by *t* test).

occurring in systemic lupus erythematosus, exert intensive soft tissue pathology marked by a presence of synovial infiltrate, edema, and joint exudate, but without the underlying bone destruction (45). Similarly, the phenotype of Fas-deficient C57BL/6 mice used in our study is characterized by lymphoproliferation and the formation of

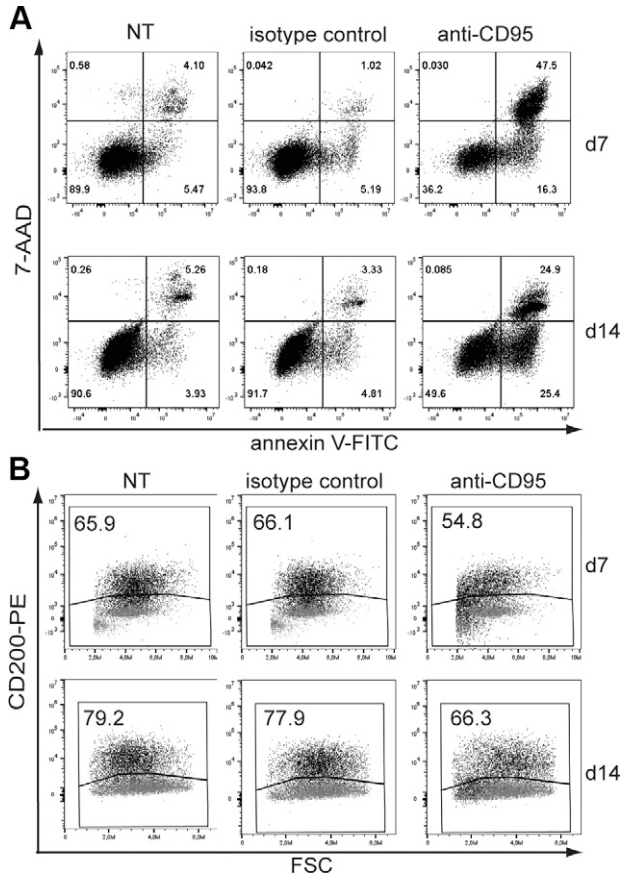

Figure 6. Susceptibility of synovial mesenchymal cells to Fas-mediated apoptosis. *A*) Representative dot plots showing proportions of apoptotic (lower right quadrant) and dead (upper right quadrant) cells, determined by labeling with Annexin V-FITC and 7-AAD. *B*) Proportion of $CD200^+$ cells among single cells, on d 7 (top row) and 14 (bottom row) in osteoblastogenic cultures from sorted synovial mesenchymal progenitors treated with 1 μg/ml anti-mouse CD95 antibody; 1 μg/ml of isotype control antibody and 1 μg/ml protein G; or only 1 μg/ml protein G (NT), on culture d 6 and 13 and harvested after 16–18 h. Experiments were repeated twice in duplicate and triplicate wells, which were pooled for analysis, and data are from representative experiment. Black dots, stained cells; red dots (overlay), nonstained cells.

autoantibodies (46), corresponding to human systemic lupus erythematosus. Despite that, Fas-deficient mice are protected from joint inflammation and subsequent bone destruction. The ability of the Fas/FasL system to induce apoptosis and to alter differentiation and the activity of bone cells has already been documented (21, 22, 25, 47), and the present study confirmed the up-regulation of the Fas receptor on the nonhematopoietic population of cells within the arthritic synovial compartment. Up-regulation of the Fas receptor on the cells of the immune system in the spleen and synovial compartment in response to immunization is an expected finding considering the well-known role of the Fas/FasL system in limiting immune activation (48–50). We previously confirmed the regulatory effect of Fas on the osteoblast lineage cells and the documented decrease in the RANKL/OPG ratio in $Fas^{-/-}$ mice with arthritis, and in this study, we further focused on the analysis of the osteoprogenitor population responsible for bone formation and for counteracting inflammation-induced increase in osteoclast differentiation and activity. Although the osteoblastogenic potential, as well as the frequency of total nonhematopoietic population containing mesenchymal progenitors is similar in the synovial compartment of WT and $Fas^{-/-}$ mice with AIA, we observed differences in the proportions of subpopulations of mesenchymal progenitors, which may implicate the specificities of a local microenvironmental control of osteoblast development and function. The proportion of $CD51^+CD200^+$ cells corresponding to earliest bone and cartilage progenitors was decreased in WT mice with AIA and was accompanied by an increase in the proportion of $CD51^+CD200^-$ cells corresponding to committed bone and cartilage progenitors (42). A decrease in the proportion of $CD51^+CD200^+$ population in WT mice with AIA and an unaffected ratio of $CD51^+CD200^-$/$CD51^+CD200^+$ cells in $Fas^{-/-}$ mice with arthritis, may reflect the removal of $CD51^+CD200^+$ by Fas-mediated apoptosis, which, in arthritis, depletes the osteoprogenitor pool and contributes to ineffective bone formation. *In vitro*, osteoprogenitors were sensitive to Fas-induced apoptosis, with more effective down-regulation of Fas with progressing maturation in the $CD51^+CD200^-$ population. A lower frequency of the earliest $CD51^+CD200^+$ progenitor cells in $Fas^{-/-}$ mice in comparison to the WT control group implies different kinetics in bone progenitor differentiation, which is further reflected by an increased proportion of committed bone progenitor $CD51^+CD200^-CD90.2^+CD105^+$ cells and suggests more-robust bone-formation potential. In addition, a recent study has shown that CD200 is required for the immunoregulatory capacity of mesenchymal cells, affecting differentiation of myeloid cells through its interaction with CD200R (51). Depletion of FasL-susceptible $CD200^+$ cells from the synovial compartment, therefore, may contribute not only to the exhaustion of the osteoprogenitor pool but also to perpetuating inflammation and, in effect, favoring the differentiation of myeloid lineage-derived osteoclasts.

In summary, the bone and cartilage progenitors in the synovial compartment represent a small but a highly adaptable population, so the preservation of the pool of the early osteoprogenitor subset in the state of Fas deficiency may represent an additional bone-protective mechanism during AIA in $Fas^{-/-}$ mice. Because Fas can induce death of these cells, further understanding of this process might reveal potential new approaches to counteract local bone destruction during arthritis. FJ

ACKNOWLEDGMENTS

The authors thank Katerina Zrinski-Petrović (Laboratory for Molecular Immunology) for her technical assistance and Ivan Krešimir Lukić (Bjelovar University of Applied Sciences, Bjelovar, Croatia) for advice regarding statistical analysis. The authors thank the Laboratory for Mineralized Tissues, School of Medicine at the University of Zagreb, for access to the 1076 SkyScan μCT instrument. This work was supported by Croatian

Science Foundation Grants 7406 and 5699, the Scientific Center of Excellence for Reproductive and Regenerative Medicine (Project "Reproductive and Regenerative Medicine–Exploration of New Platforms and Potentials") Grant KK01.1.1.01.0008, Research Centre of Excellence of Fundamental Clinical and Translational Neuroscience, and CoRE-Neuro Grant KK01.1.1.01.0007, both funded by the European Union through the European Regional Development Fund, and Croatian Ministry of Science, Education and Sports Grant 1080229-0140. The authors declare no conflicts of interest.

AUTHOR CONTRIBUTIONS

E. Lazić Mosler and N. Lukač designed and performed the research, analyzed the data, and wrote the manuscirpt; D. Flegar, M. Fadljević, I. Radanović, H. Cvija, T. Kelava, S. Ivčević, A. Šućur, and A. Markotić performed the research and analyzed the data; V. Katavić performed the research, analyzed the data, and critically revised the manuscript; A. Marušić designed the research and critically revised the manuscript; D. Grčević designed and performed the research and critically revised the manuscript; N. Kovačić designed and performed the research, analyzed the data, and wrote and critically revised the manuscript; and all authors read and approved the final version of the manuscript.

REFERENCES

1. Feldmann, M., Brennan, F. M., and Maini, R. N. (1996) Rheumatoid arthritis. *Cell* **85**, 307–310
2. McInnes, I. B., and Schett, G. (2007) Cytokines in the pathogenesis of rheumatoid arthritis. *Nat. Rev. Immunol.* **7**, 429–442
3. Furuzawa-Carballeda, J., Vargas-Rojas, M. I., and Cabral, A. R. (2007) Autoimmune inflammation from the Th17 perspective. *Autoimmun. Rev.* **6**, 169–175
4. Lotito, A. P., Silva, C. A., and Mello, S. B. (2007) Interleukin-18 in chronic joint diseases. *Autoimmun. Rev.* **6**, 253–256
5. Malemud, C. J. (2011) Dysfunctional immune-mediated inflammation in rheumatoid arthritis dictates that development of anti-rheumatic disease drugs target multiple intracellular signaling pathways. *Antiinflamm. Antiallergy Agents Med. Chem.* **10**, 78–84
6. Malemud, C. J. (2009) Recent advances in neutralizing the IL-6 pathway in arthritis. *Open Access Rheumatol.* **1**, 133–150
7. Hartgring, S. A., Bijlsma, J. W., Lafeber, F. P., and van Roon, J. A. (2006) Interleukin-7 induced immunopathology in arthritis. *Ann. Rheum. Dis.* **65** (Suppl 3), iii69–iii74
8. Petrovic-Rackov, L., and Pejnovic, N. (2006) Clinical significance of IL-18, IL-15, IL-12 and TNF-α measurement in rheumatoid arthritis. *Clin. Rheumatol.* **25**, 448–452
9. Collison, L. W., Workman, C. J., Kuo, T. T., Boyd, K., Wang, Y., Vignali, K. M., Cross, R., Sehy, D., Blumberg, R. S., and Vignali, D. A. (2007) The inhibitory cytokine IL-35 contributes to regulatory T-cell function. *Nature* **450**, 566–569
10. Bottini, N., and Firestein, G. S. (2013) Duality of fibroblast-like synoviocytes in RA: passive responders and imprinted aggressors. *Nat. Rev. Rheumatol.* **9**, 24–33
11. Walsh, N. C., and Gravallese, E. M. (2010) Bone remodeling in rheumatic disease: a question of balance. *Immunol. Rev.* **233**, 301–312
12. Schett, G. (2009) Osteoimmunology in rheumatic diseases. *Arthritis Res. Ther.* **11**, 210
13. Sućur, A., Katavić, V., Kelava, T., Jajić, Z., Kovačić, N., and Grčević, D. (2014) Induction of osteoclast progenitors in inflammatory conditions: key to bone destruction in arthritis. *Int. Orthop.* **38**, 1893–1903
14. Boyce, B. F., and Xing, L. (2008) Functions of RANKL/RANK/OPG in bone modeling and remodeling. *Arch. Biochem. Biophys.* **473**, 139–146
15. Li, X., and Makarov, S. S. (2006) An essential role of NF-kappaB in the "tumor-like" phenotype of arthritic synoviocytes. *Proc. Natl. Acad. Sci. USA* **103**, 17432–17437
16. Lazić, E., Jelušić, M., Grčević, D., Marušić, A., and Kovačić, N. (2012) Osteoblastogenesis from synovial fluid-derived cells is related to the type and severity of juvenile idiopathic arthritis. *Arthritis Res. Ther.* **14**, R139
17. Malemud, C. J. (2013) Intracellular signaling pathways in rheumatoid arthritis. *J. Clin. Cell. Immunol.* **4**, 160
18. Diarra, D., Stolina, M., Polzer, K., Zwerina, J., Ominsky, M. S., Dwyer, D., Korb, A., Smolen, J., Hoffmann, M., Scheinecker, C., van der Heide, D., Landewe, R., Lacey, D., Richards, W. G., and Schett, G. (2007) Dickkopf-1 is a master regulator of joint remodeling. *Nat. Med.* **13**, 156–163
19. Aggarwal, B. B. (2003) Signalling pathways of the TNF superfamily: a double-edged sword. *Nat. Rev. Immunol.* **3**, 745–756
20. Askenasy, N., Yolcu, E. S., Yaniv, I., and Shirwan, H. (2005) Induction of tolerance using Fas ligand: a double-edged immunomodulator. *Blood* **105**, 1396–1404
21. Kovacić, N., Lukić, I. K., Grcević, D., Katavić, V., Croucher, P., and Marusić, A. (2007) The Fas/Fas ligand system inhibits differentiation of murine osteoblasts but has a limited role in osteoblast and osteoclast apoptosis. *J. Immunol.* **178**, 3379–3389
22. Nakamura, T., Imai, Y., Matsumoto, T., Sato, S., Takeuchi, K., Igarashi, K., Harada, Y., Azuma, Y., Krust, A., Yamamoto, Y., Nishina, H., Takeda, S., Takayanagi, H., Metzger, D., Kanno, J., Takaoka, K., Martin, T. J., Chambon, P., and Kato, S. (2007) Estrogen prevents bone loss via estrogen receptor α and induction of Fas ligand in osteoclasts. *Cell* **130**, 811–823
23. Katavić, V., Lukić, I. K., Kovacić, N., Grcević, D., Lorenzo, J. A., and Marusić, A. (2003) Increased bone mass is a part of the generalized lymphoproliferative disorder phenotype in the mouse. *J. Immunol.* **170**, 1540–1547
24. Krum, S. A., Miranda-Carboni, G. A., Hauschka, P. V., Carroll, J. S., Lane, T. F., Freedman, L. P., and Brown, M. (2008) Estrogen protects bone by inducing Fas ligand in osteoblasts to regulate osteoclast survival. *EMBO J.* **27**, 535–545
25. Wu, X., McKenna, M. A., Feng, X., Nagy, T. R., and McDonald, J. M. (2003) Osteoclast apoptosis: the role of Fas *in vivo* and *in vitro*. *Endocrinology* **144**, 5545–5555
26. Calmon-Hamaty, F., Audo, R., Combe, B., Morel, J., and Hahne, M. (2015) Targeting the Fas/FasL system in rheumatoid arthritis therapy: promising or risky? *Cytokine* **75**, 228–233
27. Peng, S. L. (2006) Fas (CD95)-related apoptosis and rheumatoid arthritis. *Rheumatology (Oxford)* **45**, 26–30
28. Fujisawa, K., Asahara, H., Okamoto, K., Aono, H., Hasunuma, T., Kobata, T., Iwakura, Y., Yonehara, S., Sumida, T., and Nishioka, K. (1996) Therapeutic effect of the anti-Fas antibody on arthritis in HTLV-1 tax transgenic mice. *J. Clin. Invest.* **98**, 271–278
29. Zhang, H., Yang, Y., Horton, J. L., Samoilova, E. B., Judge, T. A., Turka, L. A., Wilson, J. M., and Chen, Y. (1997) Amelioration of collagen-induced arthritis by CD95 (Apo-1/Fas)-ligand gene transfer. *J. Clin. Invest.* **100**, 1951–1957
30. Kim, S. H., Kim, S., Oligino, T. J., and Robbins, P. D. (2002) Effective treatment of established mouse collagen-induced arthritis by systemic administration of dendritic cells genetically modified to express FasL. *Mol. Ther.* **6**, 584–590
31. Schedel, J., Gay, R. E., Kuenzler, P., Seemayer, C., Simmen, B., Michel, B. A., and Gay, S. (2002) FLICE-inhibitory protein expression in synovial fibroblasts and at sites of cartilage and bone erosion in rheumatoid arthritis. *Arthritis Rheum.* **46**, 1512–1518
32. García, S., Liz, M., Gómez-Reino, J. J., and Conde, C. (2010) Akt activity protects rheumatoid synovial fibroblasts from Fas-induced apoptosis by inhibition of Bid cleavage. *Arthritis Res. Ther.* **12**, R33
33. Tu-Rapp, H., Hammermüller, A., Mix, E., Kreutzer, H. J., Goerlich, R., Köhler, H., Nizze, H., Thiesen, H. J., and Ibrahim, S. M. (2004) A proinflammatory role for Fas in joints of mice with collagen-induced arthritis. *Arthritis Res. Ther.* **6**, R404–R414
34. Ma, Y., Liu, H., Tu-Rapp, H., Thiesen, H. J., Ibrahim, S. M., Cole, S. M., and Pope, R. M. (2004) Fas ligation on macrophages enhances IL-1R1-Toll-like receptor 4 signaling and promotes chronic inflammation. *Nat. Immunol.* **5**, 380–387
35. Huang, Q. Q., Birkett, R., Koessler, R. E., Cuda, C. M., Haines G. K. III, Jin, J. P., Perlman, H., and Pope, R. M. (2014) Fas signaling in macrophages promotes chronicity in K/BxN serum-induced arthritis. *Arthritis Rheumatol.* **66**, 68–77

36. Adachi, M., Suematsu, S., Kondo, T., Ogasawara, J., Tanaka, T., Yoshida, N., and Nagata, S. (1995) Targeted mutation in the Fas gene causes hyperplasia in peripheral lymphoid organs and liver. *Nat. Genet.* **11**, 294–300
37. Odobasic, D., Leech, M. T., Xue, J. R., and Holdsworth, S. R. (2008) Distinct in vivo roles of CD80 and CD86 in the effector T-cell responses inducing antigen-induced arthritis. *Immunology* **124**, 503–513
38. Ikić Matijašević, M., Flegar, D., Kovačić, N., Katavić, V., Kelava, T., Šućur, A., Ivčević, S., Cvija, H., Lazić Mosler, E., Kalajzić, I., Marušić, A., and Grčević, D. (2016) Increased chemotaxis and activity of circulatory myeloid progenitor cells may contribute to enhanced osteoclastogenesis and bone loss in the C57BL/6 mouse model of collagen-induced arthritis. *Clin. Exp. Immunol.* **186**, 321–335
39. Grčević, D., Sironi, M., Valentino, S., Deban, L., Cvija, H., Inforzato, A., Kovačić, N., Katavić, V., Kelava, T., Kalajzić, I., Mantovani, A., and Bottazzi, B. (2018) The long pentraxin 3 plays a role in bone turnover and repair. *Front. Immunol.* **9**, 417
40. Krause, U., Seckinger, A., and Gregory, C. A. (2011) *Mesenchymal Stem Cell Assays and Applications* (Vemuri, M. C., Chase, L. G., and and Lipnick, S., eds.), Springer, Berlin
41. Conover, W. J. (1999) *Practical Nonparametric Statistics*, 3rd ed., (Wiley, B., and and O'Sullivan, M., eds.), pp. 428–433, John Wiley & Sons, New York
42. Chan, C. K., Seo, E. Y., Chen, J. Y., Lo, D., McArdle, A., Sinha, R., Tevlin, R., Seita, J., Vincent-Tompkins, J., Wearda, T., Lu, W. J., Senarath-Yapa, K., Chung, M. T., Marecic, O., Tran, M., Yan, K. S., Upton, R., Walmsley, G. G., Lee, A. S., Sahoo, D., Kuo, C. J., Weissman, I. L., and Longaker, M. T. (2015) Identification and specification of the mouse skeletal stem cell. *Cell* **160**, 285–298
43. Kovacic, N., Grcevic, D., Katavic, V., Lukic, I. K., Grubisic, V., Mihovilovic, K., Cvija, H., Croucher, P. I., and Marusic, A. (2010) Fas receptor is required for estrogen deficiency-induced bone loss in mice. *Lab. Invest.* **90**, 402–413
44. Paquet, J., Goebel, J. C., Delaunay, C., Pinzano, A., Grossin, L., Cournil-Henrionnet, C., Gillet, P., Netter, P., Jouzeau, J. Y., and Moulin, D. (2012) Cytokines profiling by multiplex analysis in experimental arthritis: which pathophysiological relevance for articular versus systemic mediators? *Arthritis Res. Ther.* **14**, R60
45. Ostendorf, B., Scherer, A., Specker, C., Mödder, U., and Schneider, M. (2003) Jaccoud's arthropathy in systemic lupus erythematosus: differentiation of deforming and erosive patterns by magnetic resonance imaging. *Arthritis Rheum.* **48**, 157–165
46. Adachi, M., Suematsu, S., Suda, T., Watanabe, D., Fukuyama, H., Ogasawara, J., Tanaka, T., Yoshida, N., and Nagata, S. (1996) Enhanced and accelerated lymphoproliferation in Fas-null mice. *Proc. Natl. Acad. Sci. USA* **93**, 2131–2136
47. Park, H., Jung, Y. K., Park, O. J., Lee, Y. J., Choi, J. Y., and Choi, Y. (2005) Interaction of Fas ligand and Fas expressed on osteoclast precursors increases osteoclastogenesis. *J. Immunol.* **175**, 7193–7201
48. Van Parijs, L., and Abbas, A. K. (1998) Homeostasis and self-tolerance in the immune system: turning lymphocytes off. *Science* **280**, 243–248
49. Daniel, P. T., and Krammer, P. H. (1994) Activation induces sensitivity toward APO-1 (CD95)-mediated apoptosis in human B cells. *J. Immunol.* **152**, 5624–5632
50. Jagger, A. L., Evans, H. G., Walter, G. J., Gullick, N. J., Menon, B., Ballantine, L. E., Gracie, A., Magerus-Chatinet, A., Tiemessen, M. M., Geissmann, F., Rieux-Laucat, F., and Taams, L. S. (2012) FAS/FAS-L dependent killing of activated human monocytes and macrophages by CD4+CD25- responder T cells, but not CD4+CD25+ regulatory T cells. *J. Autoimmun.* **38**, 29–38
51. Amouzegar, A., Mittal, S. K., Sahu, A., Sahu, S. K., and Chauhan, S. K. (2017) Mesenchymal stem cells modulate differentiation of myeloid progenitor cells during inflammation. *Stem Cells* **35**, 1532–1541

Received for publication July 12, 2018.
Accepted for publication October 9, 2018.